Casimir effect in magnetic dual chiral density waves

Daisuke Fujii [ID],[1, 2, *] Katsumasa Nakayama [ID],[3, †] and Kei Suzuki [ID][1, ‡]

[1]*Advanced Science Research Center, Japan Atomic Energy Agency (JAEA), Tokai, 319-1195, Japan*
[2]*Research Center for Nuclear Physics, Osaka University, Ibaraki 567-0048, Japan*
[3]*RIKEN Center for Computational Science, Kobe, 650-0047, Japan*

We theoretically investigate the Casimir effect originating from Dirac fields in finite-density matter under a magnetic field. In particular, we focus on quark fields in the magnetic dual chiral density wave (MDCDW) phase as a possible inhomogeneous ground state of interacting Dirac-fermion systems. In this system, the distance dependence of Casimir energy shows a complex oscillatory behavior by the interplay between the chemical potential, magnetic field, and inhomogeneous ground state. By decomposing the total Casimir energy into contributions of each Landau level, we elucidate what types of Casimir effects are realized from each Landau level: the lowest or some types of higher Landau levels lead to different behaviors of Casimir energies. Furthermore, we point out characteristic behaviors due to level splitting between different fermion flavors, i.e., up/down quarks. These findings provide new insights into Dirac-fermion (or quark) matter with a finite thickness.

I. INTRODUCTION

The Casimir effect proposed by Casimir [1] is of great importance for understanding small-volume physics in quantum field theory. Casimir predicted that a reduction in the zero-point energy of the photon field by two parallel conducting plates in a vacuum would induce an attractive force, known as the Casimir energy or Casimir force. This theoretical prediction was experimentally confirmed several decades later [2, 3] (for reviews, see Refs. [4–11]).

While the original Casimir effect means an attractive force from the photon field in a vacuum, other types of Casimir (or Casimir-like) effects have also been explored. For example, one can consider counterparts induced by fermion fields [12, 13] such as quarks or in systems filled by a medium [14]. Such an unusual setup sometimes leads to anomalous phenomena, such as sign-flipping and oscillating behaviors of Casimir energy as a function of distance. In particular, in fermionic systems, (i) external magnetic fields[1] and (ii) chemical potentials can be experimentally tunable, so that these parameters should be useful for the controllability and versatility of the fermionic Casimir effect.

In this paper, we investigate the Casimir effect for Dirac fields under both (i) and (ii) for the first time, where we particularly focus on thin quark matter under a magnetic field (see Fig. 1). Our previous work [40] found that an *oscillating Casimir effect* is induced not

only by the quark Fermi sea but also by the dynamics of quark fields modified in the *dual chiral density wave* (DCDW) phase [41–43] which is a possible ground state of quantum chromodynamics (QCD) at finite quark chemical potential. However, the DCDW phase (more generally, an inhomogeneous phase) can exist only in a narrow density region. Therefore, in this study, we consider a more feasible situation, that is, the DCDW phase under a magnetic field. When a magnetic field is imposed on the DCDW phase, the property of the DCDW is modified, which may be called the *magnetic dual chiral density wave* (MDCDW) [44] (see Refs. [45–60] for related studies and Ref. [61] for a review). A magnetic field makes the DCDW phase more robust, and in particular, at finite temperature, it removes the Landau-Peierls instability [51]. Such robustness might support the formation of DCDW in fireballs produced by heavy-ion col-
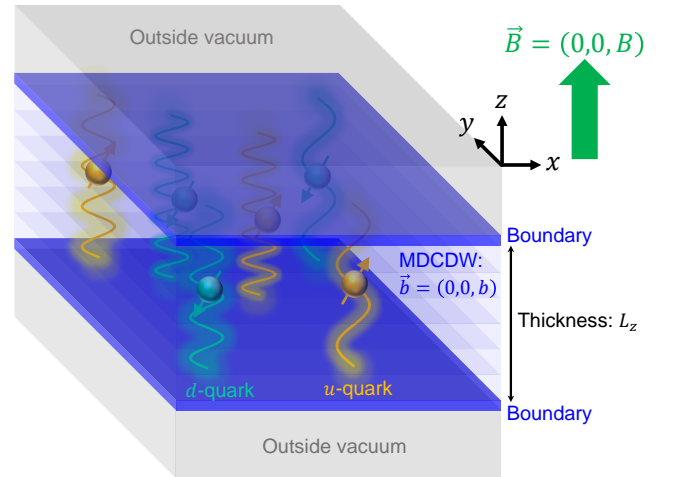

FIG. 1. Schematic picture of the Casimir effect in the two-flavor MDCDW phase, where the MDCDW phase is sandwiched by two boundary conditions at $z = 0$ and $z = L_z$. The magnetic field $\vec{B}$ and the wave number $\vec{b}$ of density waves are parallel to z the direction.

---

* daisuke@rcnp.osaka-u.ac.jp
† katsumasa.nakayama@riken.jp
‡ k.suzuki.2010@th.phys.titech.ac.jp

[1] Since the photon is not directly coupled to an external magnetic field, the magnetic response of the photonic Casimir effect in quantum electrodynamics (QED) vacuum is described as a higher-order correction due to electron-positron loops [15]. On the other hand, the Casimir effect originated from Dirac fields [16–27] (as well as charged scalar fields [19, 22, 28–39]) is directly affected by magnetic fields. Therefore, quark fields which we consider in this work can be a realistic testing ground for the Casimir effect coupled to magnetic fields.

lision experiments and in the interior of neutron stars.

This paper is organized as follows. In Sec. II, we review the MDCDW phase described by an effective model of interacting Dirac fermions and explain how to calculate Casimir energy in this phase. In Sec. III, we show our results. Sec. IV is devoted to the conclusion.

II. MODEL CONSTRUCTION

A. The model

To investigate quark matter in a magnetic field, we use the Nambu–Jona-Lasinio (NJL) model [62, 63] which is an effective model of QCD (see Refs. [64–67] for reviews). The Lagrangian density of the NJL model in a magnetic field is written as

$$\mathcal{L}_{\mathrm{NJL}} = \bar{\psi}(i\slashed{D} + \mu\gamma_0)\psi + G[(\bar{\psi}\psi)^2 + (\bar{\psi}i\gamma_5\vec{\tau}\psi)^2], \quad (1)$$

where the quark field ψ has two-flavor ($N_f = 2$) and three-color ($N_c = 3$) components, and $\mu > 0$ is the chemical potential of quarks. G is the coupling constant for the four-point interactions, and $\vec{\tau}$ is the Pauli matrix in the isospin (up or down quark) space, and γ^μ and $\gamma_5 \equiv i\gamma^0\gamma^1\gamma^2\gamma^3$ are the gamma matrix in the $3 + 1$ dimensional spacetime. The covariant derivative is defined as $\slashed{D} \equiv \gamma^\mu(\partial_\mu + iQA_\mu)$ using the gauge field A_μ and the electric-charge matrix $Q \equiv \mathrm{diag}(q_u, q_d) = \mathrm{diag}(\frac{2}{3}e, -\frac{1}{3}e)$ with the elementary charge $e > 0$. Note that, in a vanishing electromagnetic field, the model (1) satisfies the $SU(2)_L \times SU(2)_R$ chiral symmetry. When an external magnetic field is switched on, this symmetry is broken to $U(1)_L \times U(1)_R$.

As the mean-field ansatz for the DCDW phase, we adopt

$$\begin{aligned} \langle\bar{\psi}\psi\rangle &= \Delta\cos(\vec{q}\cdot\vec{r}), \quad \langle\bar{\psi}i\gamma_5\tau_3\psi\rangle = \Delta\sin(\vec{q}\cdot\vec{r}), \\ \langle\bar{\psi}i\gamma_5\tau_1\psi\rangle &= 0, \qquad \langle\bar{\psi}i\gamma_5\tau_2\psi\rangle = 0, \end{aligned} \quad (2)$$

where Δ, $\vec{q} = (0, 0, q)$, and $\vec{r} = (x, y, z)$ are the amplitude of DCDW, the wave number of DCDW propagating in the z direction, and the position vector, respectively.

Using the mean-field ansatz (2), we obtain the mean-field Lagrangian,

$$\mathcal{L}_{\mathrm{MF}} = \bar{\psi}[i\slashed{D} + \mu\gamma_0 - M(\cos qz + i\gamma_5\tau_3\sin qz)]\psi - \frac{M^2}{4G}, \quad (3)$$

where $M = -2G\Delta$.

By performing a local chiral transformation

$$\psi \to e^{i\gamma_5\tau_3 qz/2}\psi, \quad \bar{\psi} \to \bar{\psi}e^{i\gamma_5\tau_3 qz/2} \quad (4)$$

(called the Weinberg transformation), we can eliminate the position dependence in the Lagrangian. The Lagrangian is then rewritten as

$$\mathcal{L}_{\mathrm{MF}} = \bar{\psi}(i\slashed{D} + \mu\gamma_0 - M + \gamma_5\tau_3\gamma^\mu q_\mu/2)\psi - \frac{M^2}{4G}. \quad (5)$$

Assuming also that the background electromagnetic field is $A_\mu = (0, 0, Bx, 0)$ using the Landau gauge, we obtain a magnetic field $\vec{B}$ parallel to $\vec{q}$ (see Fig. 1).

From the Lagrangian (5), by diagonalizing the inverse of the quark propagator in momentum space, we obtain the following energy eigenvalues [44]:

$$\omega_{l=0} = E_{l=0} + b - \mu, \quad \tilde{\omega}_{l=0} = -E_{l=0} + b - \mu, \quad (6)$$

$$\omega_{\zeta,l} = E_{\zeta,l} - \mu, \quad \tilde{\omega}_{\zeta,l} = -E_{\zeta,l} - \mu, \quad (7)$$

$$E_{l=0} \equiv \sqrt{M^2 + k_z^2},$$

$$E_{\zeta,l} \equiv \sqrt{(\zeta\sqrt{M^2 + k_z^2} + b)^2 + 2|q_f B|l}, \quad (l = 1, 2, ...),$$

where we redefined $b_\mu \equiv q_\mu/2 = (0, 0, 0, q/2) = (0, 0, 0, b)$. ω and $\tilde{\omega}$ denote the positive and negative energy solutions (at $\mu = 0$), respectively. $\zeta = \pm$ is a spin polarization index, and $q_f = q_u$ or q_d. The presence of a magnetic field splits the eigenmodes of quarks into an infinite number of Landau levels (LLs) labeled by l. The two modes with $l = 0$, Eq. (6), are called lowest Landau levels (LLLs), and an infinite set of four modes with $l \geq 1$, Eq. (7), is called higher Landau levels (HLLs). The LLLs have no spin index because only one spin component is chosen.[2] On the other hand, HLLs have both modes with $\zeta = \pm$.

B. Casimir energy

From the partition function Z of the mean-field Lagrangian (5), the grand potential $\Omega \equiv -\frac{T}{V}\ln Z$ per unit volume $V = L_x L_y L_z$ at temperature $T = 1/\beta$ is written as [44]

$$\Omega = \Omega_{\mathrm{LLL}} + \Omega_{\mathrm{HLL}} + \frac{M^2}{4G}, \quad (8)$$

$$\begin{aligned} \Omega_{\mathrm{LLL}} = -N_c \sum_{q_f} \frac{|q_f B|}{2\pi} \int \frac{dk_z}{2\pi} \Big[&\frac{1}{2}|\omega_{l=0}| + \frac{1}{2}|\tilde{\omega}_{l=0}| \\ &+ \frac{1}{\beta}\ln\Big\{\Big(1 + e^{-\beta|\omega_{l=0}|}\Big)\Big(1 + e^{-\beta|\tilde{\omega}_{l=0}|}\Big)\Big\}\Big], \end{aligned}$$

$$\begin{aligned} \Omega_{\mathrm{HLL}} = -N_c \sum_{q_f,\zeta} \frac{|q_f B|}{2\pi} \int \frac{dk_z}{2\pi} \sum_{l=1}^{\infty} \Big[&\frac{1}{2}|\omega_{\zeta,l}| + \frac{1}{2}|\tilde{\omega}_{\zeta,l}| \\ &+ \frac{1}{\beta}\ln\Big\{\Big(1 + e^{-\beta|\omega_{\zeta,l}|}\Big)\Big(1 + e^{-\beta|\tilde{\omega}_{\zeta,l}|}\Big)\Big\}\Big], \end{aligned}$$

where $|q_f B|/2\pi$ is called the Landau degeneracy factor which is the remnant of the (k_x, k_y) integrals at $B = 0$.

---

[2] In the LLLs, Eq. (6), the asymmetry between $\omega_{l=0}$ and $\tilde{\omega}_{l=0}$ due to $b \neq 0$ is called the *spectral asymmetry* [44, 45].

In the zero-temperature limit, we obtain [44]

$$\Omega(T \to 0) = \Omega_{\mathrm{LLL}}^{T \to 0} + \Omega_{\mathrm{HLL}}^{T \to 0} + \frac{M^2}{4G} \equiv \frac{E_0^{\mathrm{int}}}{L_z}, \quad (9)$$

$$\Omega_{\mathrm{LLL}}^{T \to 0} = -N_c \sum_{q_f} \frac{|q_f B|}{2\pi} \int \frac{dk_z}{2\pi} \left(\frac{1}{2} |\omega_{l=0}| + \frac{1}{2} |\tilde{\omega}_{l=0}| \right),$$

$$\Omega_{\mathrm{HLL}}^{T \to 0} = -N_c \sum_{q_f, \zeta} \frac{|q_f B|}{2\pi} \int \frac{dk_z}{2\pi} \sum_{l=1}^{\infty} \left(\frac{1}{2} |\omega_{\zeta,l}| + \frac{1}{2} |\tilde{\omega}_{\zeta,l}| \right),$$

where we defined a new notation E_0^{int} as the zero-point energy per unit area $L_x L_y$ (not per unit volume).

The Casimir energy appears as a finite volume effect of the zero-point energy. In this work, we impose the periodic boundary conditions (PBCs) at $z = 0$ and $z = L_z$ (see Fig. 1). Then, the momentum in the z direction is discretized as $k_z \to 2n\pi/L_z$, $(n = 0, \pm 1, ..., \pm \infty)$, the momentum integral of Eq. (9) is replaced by the corresponding momentum sum. Thus, the zero-point energy at finite L_z is written as

$$E_0^{\mathrm{sum}} \equiv E_0^{\mathrm{int}}(k_z \to \tfrac{2n\pi}{L_z}) = E_{0,\mathrm{LLL}}^{\mathrm{sum}} + E_{0,\mathrm{HLL}}^{\mathrm{sum}} + \frac{M^2}{4G} L_z, \quad (10)$$

$$E_{0,\mathrm{LLL}}^{\mathrm{sum}} = -N_c \sum_{q_f} \frac{|q_f B|}{2\pi} \sum_{n=-\infty}^{\infty} \left(\frac{1}{2} |\omega_{l=0,n}| + \frac{1}{2} |\tilde{\omega}_{l=0,n}| \right),$$

$$E_{0,\mathrm{HLL}}^{\mathrm{sum}} = -N_c \sum_{q_f, \zeta} \frac{|q_f B|}{2\pi} \sum_{l=1}^{\infty} \sum_{n=-\infty}^{\infty} \left(\frac{1}{2} |\omega_{\zeta,l,n}| + \frac{1}{2} |\tilde{\omega}_{\zeta,l,n}| \right).$$

In this work, unlike the conventional mean-field approach in the NJL model, we do not minimize the thermodynamic potential (or solve the gap equation) at finite L_z. Instead, we fix the values of the order parameters and then investigate what types of behaviors of the Casimir energy can be realized under a parameter set. Note that the Casimir energy appears also from the L_z dependence of the term with $M^2/4G$, but it will be neglected in our definition of Casimir energy. This is because this contribution is just the free energy shift by the L_z dependence of the order parameter M and is not directly regarded as the fermionic Casimir effect.

The infinite sum (10) contains an ultraviolet divergence, but it becomes finite by using a regularization scheme. Here we apply the Lifshitz formula [68], which was first proposed for the conventional photonic Casimir effect and is well known nowadays. Our previous works established analogous formulas for the DCDW-type dispersion relation ($M \neq 0, b \neq 0$) [40] and at finite chemical potential ($\mu \neq 0$) [69]. Using this formula, the Casimir energy for fermion fields in the MDCDW phase (i.e.,

$M \neq 0, b \neq 0, \mu \neq 0, B \neq 0$) is written as[3]

$$E_{\mathrm{Cas}} = -2N_c \int_{-\infty}^{\infty} \frac{d\xi}{2\pi} \sum_{q_f, \zeta} \sum_{l=0}^{\infty}{}' \frac{|q_f B|}{2\pi} \ln \left[1 - e^{-L_z \tilde{k}_z^{[l,\zeta]}} \right], \quad (11)$$

$$\tilde{k}_z^{[l,\zeta]} = \sqrt{ M^2 - \left(b + \zeta \sqrt{(i\xi + \mu)^2 - 2|q_f B|l} \right)^2 },$$

where the overall factor of 2 means the factor from the PBCs. The integration variable ξ is the imaginary part of the imaginary energy $i\xi$. The prime in the sum means that the factor $1/2$ is multiplied only for $l = 0$. This formula is regarded as the infinite sum of a (quasi-)one-dimensional analog of the Lifshitz formula because of the absence of the transverse-momentum integral. Also, taking the $B \to 0$ limit of Eq. (11) leads to the Casimir energy in the usual DCDW phase (i.e., $M \neq 0, b \neq 0, \mu \neq 0$),[4]

$$E_{\mathrm{Cas}}(B \to 0) =$$
$$- 2N_f N_c \int_{-\infty}^{\infty} \frac{d\xi}{2\pi} \sum_{\zeta = \pm} \int \frac{dk_x dk_y}{(2\pi)^2} \ln \left[1 - e^{-L_z \tilde{k}_z^{[\zeta]}} \right], \quad (12)$$

$$\tilde{k}_z^{[\zeta]} = \sqrt{ M^2 - \left(b + \zeta \sqrt{(i\xi + \mu)^2 - k_x^2 - k_y^2} \right)^2 }.$$

As another approach to calculate the Casimir energy, we use the lattice regularisation scheme [24, 40, 69–81]. By replacing the continuous momentum k_z in the zero-point energy (9) per unit area as $k_z \to (2 - 2\cos ak_z)/a^2$ where a is the lattice spacing in the z direction, the Casimir energy on the lattice is defined as

$$E_{\mathrm{Cas}}^{\mathrm{Lat}} = E_0^{\mathrm{sum}} - E_0^{\mathrm{int}}, \quad (13)$$

where the sum of n is restricted within the first Brillouin zone (BZ): $n = 0, 1, ..., N_z - 1$ with the number of lattice cells $N_z \equiv L_z/a$. By taking the continuum limit $a \to 0$ (i.e., by using a sufficiently small a), we can get the correct Casimir energy.

Finally, we define a Casimir coefficient,

$$C_{\mathrm{Cas}}^{[d]} = L_z^d E_{\mathrm{Cas}}/\Lambda^{3-d}. \quad (14)$$

Since now E_{Cas} is defined as a quantity with the mass dimension 3, $L_z^d E_{\mathrm{Cas}}$ is dimensionless only when $d = 3$. Therefore, we define a dimensionless quantity divided by Λ^{3-d}, where Λ is a parameter with mass dimension one. On the other hand, in a nonzero magnetic field, since

———————

[3] If $b = \mu = 0$, $M \neq 0$, and $B \neq 0$, Eq. (11) is equivalent to the known formula for the massive Dirac field in a magnetic field [16] obtained from the proper-time regularization, except for the color and flavor factors.

[4] Note that Eq. (12) was not given in our previous paper [40]. By substituting $\mu = 0$ into Eq. (12), we obtain Eq. (11) in Ref. [40].

each LL is regarded as a particle moving in the quasi-one-dimensional space, the corresponding Casimir energy may scale as $E_{\text{Cas}} \sim 1/L_z$. Therefore, in the following, $C_{\text{Cas}}^{[1]}$ will be used to characterize the Casimir energies decomposed in each LL, while $C_{\text{Cas}}^{[3]}$ will be used to characterize the total Casimir energy summed over all the LLs.

C. Classification of dispersion relations

In the presence of a magnetic field, the quark energy levels split into the infinite number of Landau levels. If the homogeneous chiral condensate phase is realized, all the HLLs behave as quasi-one-dimensional massive (or gapped) dispersion relations. In the case of the MD-CDW phase, the low-energy dispersion relations of HLLs are distorted and different from the usual massive one, which is a remnant of dispersion relations with the two Weyl points characterizing the DCDW phase in a zero magnetic field. In a weak magnetic field, lower-l (i.e., occupied) modes in the HLLs produce Fermi points (FPs). As the magnetic field increases, the spacing between $\omega_{\pm,l}$ and $\tilde{\omega}_{\pm,l}$ with the same l becomes large. $\omega_{\pm,l}$ near the Fermi level begin to exceed the Fermi level sequentially, and eventually at a strong magnetic field, all $\omega_{\pm,l}$ exceed the Fermi level, which means that there are no FPs.

In Fig. 2, we show the dispersion relations (6) and (7) at $M/\Lambda = 0.1$, $b/\Lambda = 0.5$, and $\mu/\Lambda = 0.7$ under a magnetic field $eB/\Lambda^2 = (0.1)^2$. Here, for simplicity, we consider the one-flavor case with an electric charge $q_f = \pm e$, which can be regarded as a (quasi-)electron or positron system. The choice of these parameters realizes the DCDW phase in a magnetic field, i.e., the MDCDW phase. The two solid black lines are the upper and lower modes of the LLLs. The other colored lines and the black dashed lines are the HLLs, which split the eigenmodes of the HLLs for the two spin degrees of freedom. The circles, diamonds, and triangles represent FPs. In the case of the black dashed line, there is no FP because the gap between the positive and negative energy modes spreads as l increases.

We have shown in the previous work [40] that FPs induce an oscillation in the Casimir energy. Under magnetic fields, the presence of FPs also results in the oscillating Casimir energy in the same way. In the case of current parameters, the LLLs have FPs and induce an oscillation of Casimir energy. Its oscillation period is determined by the momenta of FPs:

$$L_z^{\text{osc}} = \frac{2\pi}{|k_z^{\text{FP}}|}, \quad \left(k_z^{\text{FP}} = \pm\sqrt{(\mu - b)^2 - M^2} \right) \quad (15)$$

when the PBC is applied.[5] Thus, the necessary condition

---

[5] For the MIT bag boundary condition leading to $k_z \rightarrow (n + 1/2)\pi/L_z$ ($n = 0, 1, 2, \ldots$), the oscillation period becomes the half of that with the PBC.

$eB/\Lambda = (0.1)^2$, $M/\Lambda = 0.1$, $b/\Lambda = 0.5$, $\mu/\Lambda = 0.7$
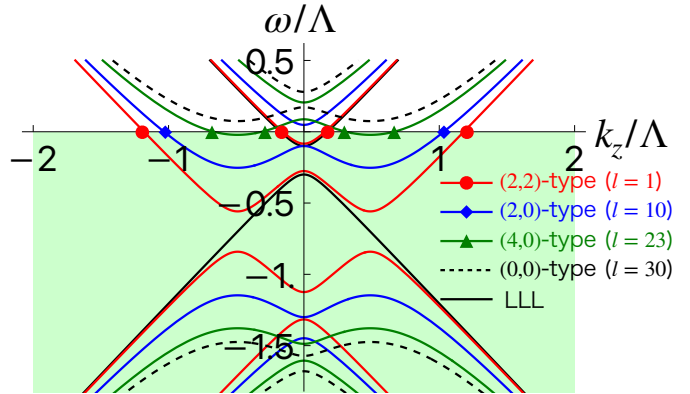

FIG. 2. Typical examples of dispersion relations for the LLLs (solid black line) and HLLs (red, blue, green, or dashed black line) of fermion fields in the MDCDW phase. Filled symbols stand for crossing points with the Fermi level, namely the Fermi points (FPs).

for this oscillation is the presence of FPs, i.e., $(\mu - b)^2 > M^2$.

For the HLLs in the MDCDW phase, we can classify possible dispersion relations into four types. Their typical forms are shown in Fig. 2.

(a) (2,2)-type: This type is realized when the condition $2|q_f B|l < (\mu^2 - (M+b)^2)$ is satisfied: the magnetic field and the label of LLs are small enough. In this type, the upper energy mode ω_+ makes two FPs, and the lower energy mode ω_- also makes two FPs. We call this type of dispersion relation the $(2,2)$-type, since both the modes make two FPs. The momentum of FPs is given as

$$|k_{z,\pm}^{\text{FP}}| = \sqrt{\left(\sqrt{\mu^2 - 2|q_f B|l} \pm b\right)^2 - M^2}. \quad (16)$$

We note that $|k_{z,+}^{\text{FP}}| > |k_{z,-}^{\text{FP}}|$, where $|k_{z,+}^{\text{FP}}|$ and $|k_{z,-}^{\text{FP}}|$ correspond to ω_- and ω_+, respectively. The resulting Casimir energy is a superposition of two oscillations with different periods ($L_z^{\text{osc}} = 2\pi/|k_{z,+}^{\text{FP}}|$ and $L_z^{\text{osc}} = 2\pi/|k_{z,-}^{\text{FP}}|$).

(b) (2,0)-type: This type is realized when the condition $(\mu^2 - (M+b)^2) < 2|q_f B|l < (\mu^2 - (M-b)^2)$ is satisfied, where only the lower mode ω_- makes two FPs. We call this type of dispersion relation the $(2,0)$-type, since only ω_- make two FPs. The resulting Casimir energy show an oscillation with a period ($L_z^{\text{osc}} = 2\pi/|k_{z,+}^{\text{FP}}|$) due to the FPs $|k_{z,+}^{\text{FP}}|$ made by ω_-.

(c) (4,0)/"Island"-type:[6] This type is realized when

---

[6] When $M \geq b$, this type is forbidden by the property of quartic functions. We will see this situation later.

TABLE I. Classification of dispersion relations possible in the MDCDW phase at $\mu > 0$: two types of LLLs and four types of HLLs, where we also list the modes with FPs, the number of induced oscillations, the classification of Casimir effect, and the oscillation period. $\omega_{l=0}$ and $\omega_{\pm,l}$ are defined as Eqs. (6) and (7). The form of L_z^{osc} is given in Eqs. (15) and (16).

Dispersion-type	Condition	with FPs	No. of osc.	Casimir effect	L_z^{osc} for PBC
LLL/"Metal"	$M^2 < (\mu - b)^2$	$\omega_{l=0}$	1	singly oscillating	$\frac{2\pi}{|k_z^{\mathrm{FP}}|}$
LLL/"Insulator"	$(\mu - b)^2 < M^2$	No	0	non-oscillating	No
(2,2)/"Metals"	$2|q_f B|l < \mu^2 - (M + b)^2$	$\omega_{-,l}, \omega_{+,l}$	2	dually oscillating	$\frac{2\pi}{|k_{z,\pm}^{\mathrm{FP}}|}$ for $\omega_{\mp,l}$
(2,0)/"Metal-Insulator"	$\mu^2 - (M + b)^2 < 2|q_f B|l < \mu^2 - (M - b)^2$	$\omega_{-,l}$	1	singly oscillating	$\frac{2\pi}{|k_{z,+}^{\mathrm{FP}}|}$
(4,0)/"Island"	$\mu^2 - (M - b)^2 < 2|q_f B|l < \mu^2$	$\omega_{-,l}$	2	dually oscillating	$\frac{2\pi}{|k_{z,+}^{\mathrm{FP}}|}, \frac{2\pi}{|k_{z,-}^{\mathrm{FP}}|}$
(0,0)/"Insulators"	$\mu^2 < 2|q_f B|l$	No	0	sign-flipping	No

TABLE II. Classification of dispersion relations of the LLLs and HLLs in the *homogeneous-chiral-condensate* phase (or massive-Dirac-fermion vacuum/matter) in a magnetic field and at $\mu > 0$. The notations are the same as those in Table I.

Dispersion-type	Condition	with FPs	No. of osc.	Casimir effect	L_z^{osc} for PBC
LLL/"Metal"	$M^2 < \mu^2$	$\omega_{l=0}$	1	singly oscillating	$\frac{2\pi}{|k_z^{\mathrm{FP}}|}$ at $b = 0$
LLL/"Insulator"	$\mu^2 < M^2$	No	0	non-oscillating	No
HLL/"Metal"	$M^2 + 2|q_f B|l < \mu^2$	$\omega_{\pm,l}$ (degenerate)	1	singly oscillating	$\frac{2\pi}{|k_{z,\pm}^{\mathrm{FP}}|}$ at $b = 0$
HLL/"Insulator"	$\mu^2 < M^2 + 2|q_f B|l$	No	0	non-oscillating	No

the condition $(\mu^2 - (M - b)^2) < 2|q_f B|l < \mu^2$ is satisfied, where the lower mode ω_- has four FPs. We call this type of dispersion relation the $(4,0)$-type or "Island"-type[7] since only the ω_- mode has the four FPs. The resulting Casimir energy is a superposition of oscillations of two different periods due to the FPs $|k_{z,\pm}^{\mathrm{FP}}|$ with $|k_{z,+}^{\mathrm{FP}}| > |k_{z,-}^{\mathrm{FP}}|$ made by ω_-.

(d) $(0,0)$-type: This type is realized when the condition $2|q_f B|l > \mu^2$ is satisfied: the magnetic field and/or the label of LLs is large enough. In this type, the lower mode ω_- is located above the Fermi level, so that there is no FP. Therefore, we call this type of dispersion relation the $(0,0)$-type. The resulting Casimir energy does not oscillate.

Finally, in Table I, we summarize the dispersion relations of LLLs and HLLs in the MDCDW phase and the properties of corresponding Casimir energy. As a comparison, in Table II, we summarize the case of the homogeneous-chiral-condensate phase (which is also regarded as just the massive-Dirac-fermion vacuum/matter) under a magnetic field. Thus, only the difference in the LLLs is the factor b, while the Casimir effects from the HLLs are drastically modified by the MD-CDW.

III. RESULTS

In this section, we discuss the Casimir energy of the MDCDW phase. In our previous work [40], we discussed the Casimir effect in the DCDW phase (without a magnetic field) and proposed that oscillating Casimir energy is produced in this phase. The origin of this effect is that the dispersion relations of quarks have Fermi points. The presence of Fermi points means that the absolute value of a dispersion relation, i.e., $|\omega|$ or $|\tilde{\omega}|$, has a nondifferentiable point in momentum space.

In this section, we adopt $\Lambda = 860$ MeV and $\hbar c \sim 197.327$ MeV $\cdot$ fm, where $\hbar$ is the reduced Planck constant and c the speed of light.

A. Casimir energy in MDCDW for one-flavor case

In this subsection, we consider the one-flavor case as a demonstration, where we use Eq. (6) and (7) with $q_f = \pm e$ as the energy eigenvalues. Based on the understanding of the dispersion relation described here and the corresponding Casimir energy, we will discuss the more realistic two-flavor case in the next subsections.

In Fig. 3 (a), we show the dispersion relations in a DCDW phase characterized by $(M/\Lambda, b/\Lambda, \mu/\Lambda) = (0.05, 0.25, 0.5)$ at $eB/\Lambda^2 = (0.05)^2$. Fig. 3 (b) shows the corresponding Casimir coefficients $C_{\mathrm{Cas}}^{[1]}$, where we separately plot the contributions from each Landau level.[8]

---

[7] "Island" means a bump structure located on the Fermi sea.

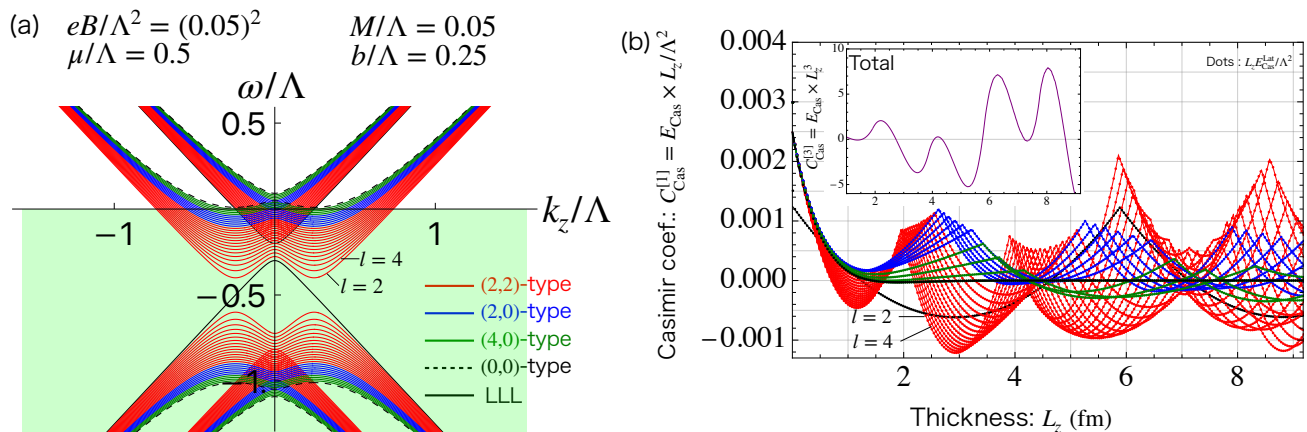[8] In this plot, the contribution of the LLLs means the sum of

FIG. 3. (a) Dispersion relations of fermion fields in the *one-flavor* MDCDW phase. (b) Thickness dependence of Casimir coefficients $C_{\text{Cas}}^{[1]}$ for each LL. Inset: the total Casimir coefficients $C_{\text{Cas}}^{[3]}$.

The inset of Fig. 3 (b) shows the total Casimir coefficients $C_{\text{Cas}}^{[3]}$ obtained by summing sufficiently many LLs. The solid lines and the dots are the results from the Lifshitz formula (11) and the lattice regularization (13), respectively.

For the LLLs, the dispersion relations and the Casimir coefficient are shown as the solid black lines in Fig. 3 (a) and (b), respectively. We find that the $C_{\text{Cas}}^{[1]}$ shown in the Fig. 3 (b) oscillate with respect to L_z. This is due to the presence of FPs created by $\omega_{l=0}$, as explained in the previous section. Its oscillation period is determined by the position of the FPs, and from Eq. (15), we can estimate $L_z^{\text{osc}} = 5.89$ fm.

For the HLLs, the behaviors of the Casimir coefficients are classified as the following four patterns.

1. $l = 1$–31 [$(2, 2)$-type]. In this type, the Casimir coefficient behaves as the superposition of oscillations with two different periods. In Fig. 3 (a), we show the quark dispersion relations of $l = 2, 4, \ldots, 30$ as the solid red lines. We can see that each mode of ω_+ or ω_- has two FPs. The periods of oscillations read from Fig. 3 (b) coincide with Eq. (16) using FPs positions in Fig. 3 (a).

2. $l = 32$–42 [$(2, 0)$-type]. In this case, the Casimir coefficient oscillates with one period. We show the quark dispersion relations of $l = 32, 34, \ldots, 42$ as the blue solid lines in Fig. 3 (a).

3. $l = 43$–50 [$(4, 0)$/Island-type]. In this case, the Casimir coefficient is a superposition of oscillations with two different periods. We show the quark dispersion relations of $l = 44, 46, 48, 50$ as the green

---

the Casimir energies from the two modes, $\omega_{l=0}$ and $\tilde{\omega}_{l=0}$. The contribution from the HLLs with $l \neq 0$ means the sum of the Casimir energies from the four modes, $\omega_{+,l}$, $\omega_{-,l}$, $\tilde{\omega}_{+,l}$, and $\tilde{\omega}_{-,l}$.

solid lines in Fig. 3 (a). We can see that ω_- has four FPs.

4. $l \geq 51$ [$(0, 0)$-type]. In this case, the Casimir coefficient does not oscillate and damps (see Sec. III D for its sign-flipping behavior). This is because every $\omega_\pm$ is located above the Fermi level.

Furthermore, we find that at $L_z \sim 0$ the amplitude of the Casimir energy from the LLLs is half of that from HLLs. This is because the eigenmodes of the LLLs pick up one spin component whereas the HLLs have two spin components. Thus, in this strength of magnetic field, the contribution from the HLLs is more dominant than that from the LLLs. Also, the result for each LL approach to a constant

$$C_{\text{Cas,LLL}}^{[1]}(L_z \to 0) = N_c \times \frac{|q_f B|}{2\pi \Lambda^2} \times \frac{\pi}{3}, \qquad (17)$$

$$C_{\text{Cas,HLL}}^{[1]}(L_z \to 0) = N_c \times \frac{|q_f B|}{2\pi \Lambda^2} \times \frac{2\pi}{3}, \qquad (18)$$

where $|q_f B|/2\pi$ is the Landau degeneracy factor [appearing as the coefficient in the thermodynamic potential (8) or the Lifshitz formula (11)], and $\pi/3$ or $2\pi/3$ is the factor known in the Casimir energy from the massless Dirac field (without or with the spin degrees of freedom 2) in the 1+1 dimensional spacetime with the PBC in one direction. In the current parameters, we get $C_{\text{Cas,LLL}}^{[1]} \to 0.00125$ and $C_{\text{Cas,HLL}}^{[1]} \to 0.0025$.

The total Casimir coefficient $C_{\text{Cas}}^{[3]}$, which is calculated by summing a sufficient number of LLs ($l_{\text{max}} = 1000$), is shown in the inset of Fig. 3 (b). In a sufficiently weak magnetic field, the total Casimir energy roughly agrees with that obtained from the three-dimensional Lifshitz formula (12). On the other hand, when L_z is small, the two Casimir energies do not coincide. This is because the HLLs become nonnegligible at small L_z, meaning that the number of LLs summed up is insufficient. In Appendix A, we examine the l_{max} dependence in the short-L_z region.
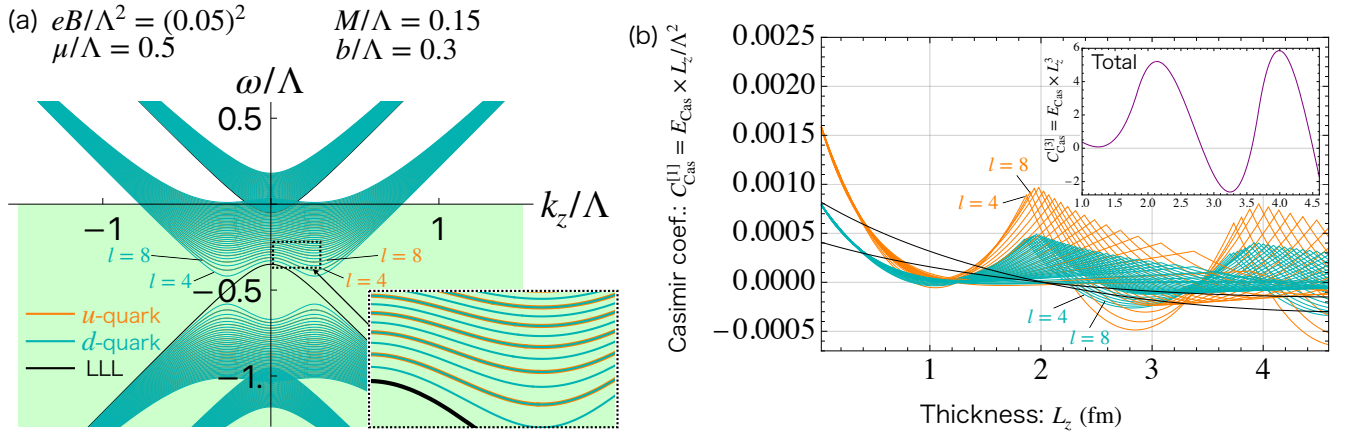
FIG. 4. (a) Dispersion relations of fermion fields in the two-flavor MDCDW phase under a *weak* magnetic field $eB/\Lambda^2 = (0.05)^2$. (b) Thickness dependence of Casimir coefficients $C_{\text{Cas}}^{[1]}$ for each LL. Inset: the total Casimir coefficient $C_{\text{Cas}}^{[3]}$.

Finally, we comment on the energy scale of our Casimir energy. As a reference, in the massless-quark vacuum (i.e., at $M = b = \mu = B = 0$), we know $C_{\text{Cas}}^{[3]} = N_f N_c \times 2\pi^2/45 \sim 2.63$ at any L_z. Then, at $L_z = 1$ fm, $E_{\text{Cas}} = C_{\text{Cas}}^{[3]} \times \hbar c/L_z^3 \sim 519$ MeV/fm$^2 \sim 8.32 \times 10^4$ N/fm, and at $L_z = 10$ fm, $E_{\text{Cas}} \sim 0.519$MeV/fm^2. The total Casimir energy in Fig. 3 (b) is about $C_{\text{Cas}}^{[3]} \sim 5$ (even in the longer L_z), which is comparable with that in the massless-quark vacuum. The emergence of the energy scale in the longer L_z is caused by the combination of the quantum effect and the finite-density effect (for the zero-density case, see Sec. III D). In addition, it may be instructive to discuss the energy scale of the Casimir energy *from each LL* in Fig. 3 (b). Then, we can estimate $C_{\text{Cas}}^{[1]} \sim 0.001$. This value is transformed to $E_{\text{Cas}} \sim 0.001 \times \Lambda^2/L_z\hbar c = 3.75$ MeV/fm^2 at $L_z = 1$ fm and $E_{\text{Cas}} \sim 0.375$ MeV/fm^2 at $L_z = 10$ fm. Therefore, E_{Cas} of each LL at $L_z \sim 10$ fm is comparable to that in the massless-quark vacuum at $L_z \sim 10$ fm.

B. Casimir energy in MDCDW (weak eB)

In the following, we consider the two-flavor case, which is more realistic as quark matter containing u and d quarks. According to Ref. [44], the DCDW phase (characterized by $M \neq 0$ and $b \neq 0$) is more stable than the homogeneous chiral-condensate phase ($M \neq 0$ and $b = 0$) if both the chemical potential μ and the magnetic field B are nonzero. Therefore, in this work, we consider only the MDCDW phase at $\mu \neq 0$ and $B \neq 0$ and do not consider the homogeneous chiral-condensate phase at $\mu \neq 0$ and $B \neq 0$.

First, we discuss the DCDW phase under a weak magnetic field. As a parameter set characterizing the MD-CDW phase, we adopt $(M/\Lambda, b/\Lambda, \mu/\Lambda) = (0.15, 0.3, 0.5)$ and $eB/\Lambda^2 = (0.05)^2$ which is determined by solving a gap equation in Ref. [44].[9] In this case, the dispersion relations for the LLLs and HLLs ($l = 4, 8, \ldots$) are shown in Fig. 4 (a). From this figure, in the case of the u quark (plotted as the orange lines), the LLs of $l = 1$–47 belong to the $(2, 2)$-type, $l = 48$–62 to the $(2, 0)$-type, $l = 63$–75 to the $(4, 0)$/Island-type, and $l > 75$ to the $(0, 0)$-type. From Eq. (7), in general, for the two-flavor case, an even number of l in the HLL dispersion relations for d quarks completely coincides with the dispersion relation for u quarks. In the case of d quarks (the green lines), the LL of $l = 1$–95 belongs to the $(2, 2)$-type, $l = 96$–126 to the $(2, 0)$-type, $l = 127$–150 to the $(4, 0)$/Island-type, and $l > 150$ to the $(0, 0)$-type. Fig. 4 (b) shows the $C_{\text{Cas}}^{[1]}$ for each of LLs and the total $C_{\text{Cas}}^{[3]}$ summing the sufficient number of LLs. Here, each line of $C_{\text{Cas}}^{[1]}$ corresponds to the dispersion relation plotted in Fig. 4 (a).

In the case of the LLLs, the dispersion relations of the u and d quarks are degenerate. The period of each $C_{\text{Cas}}^{[1]}$ is estimated to be $L_z^{\text{osc}} = 10.90$ fm from Eq. (15). Thus, the oscillation period is independent of the flavor, but due to the difference between the electric charges in the Landau degeneracy factor $|q_f B|/2\pi$, the amplitude of Casimir energy is different: The Casimir energy created by the u quark is exactly twice as large as that by the d quark.

In the case of the HLLs, the Casimir energy created by each of the u, d quarks behaves as explained in Sec. III A. Due to the difference in the electric charge, the position of the FPs, $|k_z^{\text{FP}}|$, for the u quarks labeled by l is always smaller than that for the d quarks labeled by the same l. Consequently, the oscillation period becomes longer. Also, similar to the discussion for the LLLs, due to the

_____

[9] See Fig. 2 (c) in Ref [44], where the coupling constant of the NJL model is supercritical: at $B = 0$ and a smaller μ, the chiral symmetry is broken ($M \neq 0$). In the nonzero-B and intermediate-μ region, the MDCDW phase is realized.
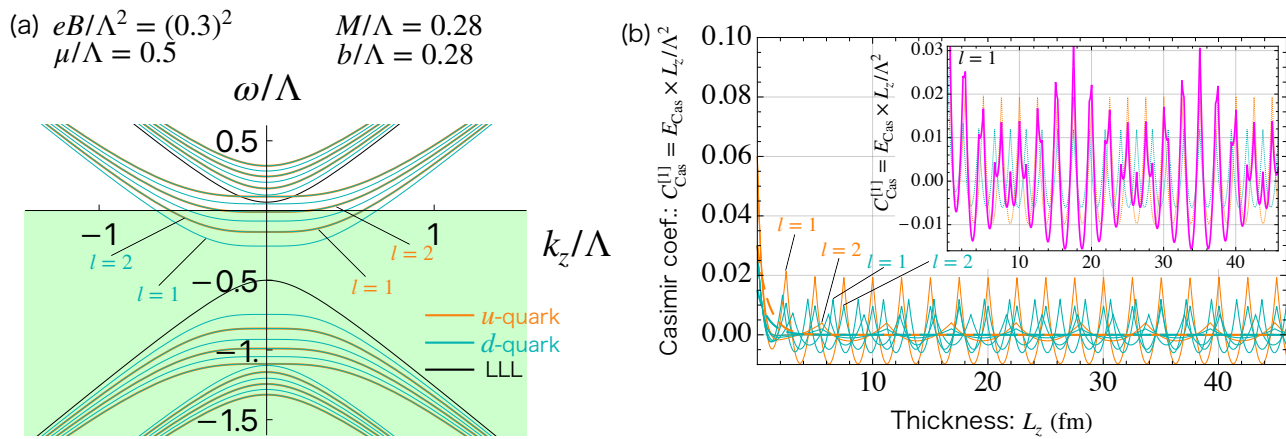
FIG. 5. (a) Dispersion relations of fermion fields in the two-flavor MDCDW phase under an *intermediate* magnetic field $eB/\Lambda^2 = (0.3)^2$. (b) Thickness dependence of Casimir coefficients $C_{\text{Cas}}^{[1]}$ from each LL. Inset: the sum of Casimir coefficients $C_{\text{Cas}}^{[1]}$ from u and d quarks at $l = 1$.

difference in the Landau degeneracy factor, the Casimir energy produced by the u quark is roughly twice as large as that produced by the d quark.

C. Casimir energy in MDCDW (intermediate eB)

As an intermediate magnetic field, we adopt $(M/\Lambda, b/\Lambda, \mu/\Lambda) = (0.28, 0.28, 0.5)$ and $eB/\Lambda^2 = (0.3)^2$ as a solution obtained in Ref. [44]. As the magnetic field increases, the upper dispersion relations $\omega_{\pm,l}$ of HLLs with higher l are above the Fermi level (the lower dispersion relations $\tilde{\omega}_{\pm,l}$ are still below the Fermi level). Since $\omega_{+,l}$ does not have FPs, there is no $(2,2)$-type dispersion relation in the current parameter set.

In this case, the dispersion relations for the LLLs and the HLLs ($l = 1, 2, ...$) are shown in Fig. 5 (a). From this figure, in the case of u quark, the LLs of $l = 1, 2$ belong to the $(2, 0)$-type, no LL to the $(4, 0)$/Island-type, and $l > 2$ to the $(0, 0)$-type. In the case of d quark, the LL of $l = 1$–4 belongs to the $(2, 0)$-type, the no LL to the $(4, 0)$/Island-type and the LL of $l > 4$ to the $(0, 0)$-type. As mentioned in footnote 6, when $M \geq b$, the $(4, 0)$/Island-type is forbidden by the property of quartic functions. The Casimir coefficient $C_{\text{Cas}}^{[1]}$ from each of LLs at $l = 1, 2$ is shown in Fig. 5 (b).

For the current parameters, the dispersion relations of the LLLs do not intersect with the Fermi level, and hence no oscillation of Casimir energy arises, which is the same as the Casimir energy for a one-dimensional massive Dirac field (with no spin degrees of freedom 2).[10] This

can be understood from the fact that the eigenvalue (6) is formally the same as that of the ordinary one-dimensional massive Dirac field shifted by $b - \mu$.

Here, we focus on only $l = 1$ of the HLLs. In the inset of Fig. 5 (b), we show the Casimir energy from each of the u, d quarks at $l = 1$ and the sum of them (the magenta line). For the current parameters, the oscillation periods of Casimir energies produced by the u, d quarks are very close to each other. Then, the superposition of the two different oscillations leads to a longer periodicity of the Casimir energy, i.e., a beating behavior with a period L_z^{beat} estimated by $1/L_z^{\text{beat}} = 1/|L_z^{\text{osc},u}| - 1/|L_z^{\text{osc},d}|$. This is a new type of *beating Casimir effect* in the sense that it originates from the flavor-dependent splitting by a magnetic field.[11] Note that this beating behavior is realized when we focus on a LL index (now, $l = 1$), but in general, the oscillatory behavior of the total Casimir energy should be more complex due to contamination of oscillations from other LLs. In the current parameters, since the LLL and HLLs of $l > 3$ for the u quark and $l > 5$ for the d quark and do not induce any oscillations, the total oscillation consists of the superposition of oscillatory behaviors of lower six levels.

D. Casimir energy in MDCDW (strong eB)

Finally, we discuss the behavior in the strong-magnetic-field region. In this subsection, we adopt $(M/\Lambda, b/\Lambda, \mu/\Lambda) = (0.57, 0.48, 0.5)$ and $eB/\Lambda^2 = (0.8)^2$ as a solution obtained in Ref. [44]. In this case, the dispersion relations for the LLLs and the HLLs with

---

[10] Its Casimir coefficient is given as the well-known formula

$$C_{\text{Cas,LLL}}^{[1]} = N_c \times \frac{|q_f B|}{2\pi\Lambda^2} \times \frac{2ML_z}{\pi} \sum_{m=1}^{\infty} \frac{K_1(mML_z)}{m}, \quad (19)$$

where K_1 is the modified Bessel function.

[11] As other examples of the beating Casimir effect, it is induced also by spin-split Dirac points [24], multiple exceptional points [78], or multiple chemical potentials [69].
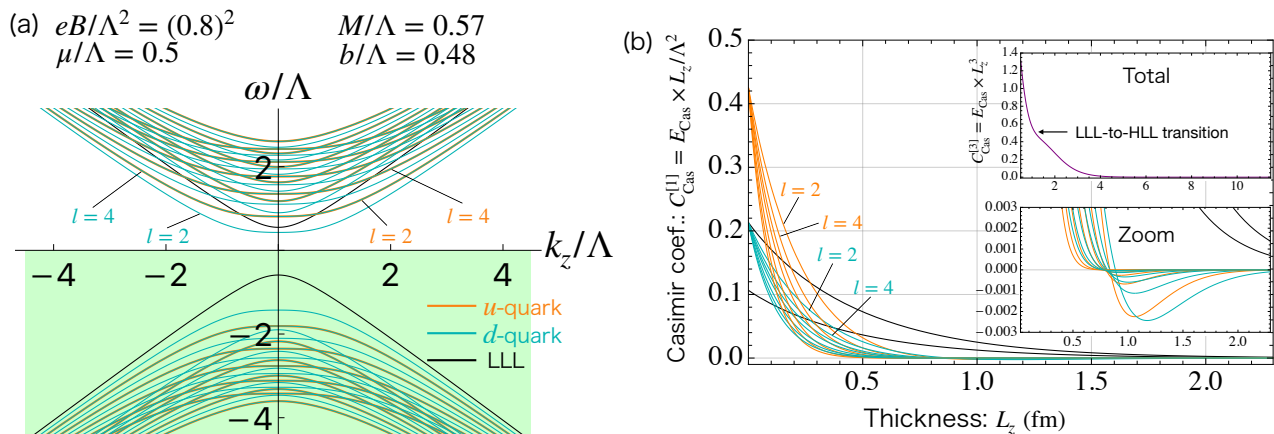
FIG. 6. (a) Dispersion relations of fermion fields in the two-flavor MDCDW phase under a *strong* magnetic field $eB/\Lambda^2 = (0.8)^2$. (b) Thickness dependence of Casimir coefficients $C_{\text{Cas}}^{[1]}$ for each LL. Upper inset: the total Casimir coefficients $C_{\text{Cas}}^{[3]}$. Lower inset: a close-up view near the $C_{\text{Cas}}^{[1]} = 0$.

$l = 2, 4, \ldots$ are shown in Fig. 6 (a). For both the u, d quarks, the dispersion relations for all HLLs belong to the $(0, 0)$-type, which means that all the HLLs do not cross the Fermi level. Figure 6 (b) shows $C_{\text{Cas}}^{[1]}$ from each of the LLs.

In this parameter set, the dispersion relations of all the LLs do not cross the Fermi level, and hence do not induce any oscillating behavior of Casimir energy. In particular, the functional form of Casimir energies for the LLLs is the same as that from ordinary one-dimensional massive Dirac fields.

We find that, in the short-L_z region, the contribution of HLLs is not negligible. On the other hand, in the long-L_z region, the Casimir energy for the HLLs rapidly decreases, so that the total Casimir energy is dominated by the LLLs. Also, we find that the signs of Casimir energy for HLLs change near $L_z \sim 0.8$ fm and then damps, as shown in the lower inset of Fig. 6 (b). Such a *sign-flipping Casimir effect* is distinct from the case of the LLLs, which originates from the functional form of the eigenvalues (7) of HLLs.[12]

In addition, we can find a transition of the total $C_{\text{Cas}}^{[3]}$ at $L_z \sim 1$ fm, where the Casimir energy switches from the region dominated by the LLLs to that dominated by HLLs, which may be called the *LLL-to-HLL transition*. This transition was first discovered by the formula

for the massive Dirac field under a magnetic field in the early study [18]. Since the LLL-to-HLL transition is a property for the normal massive Dirac field, there is no direct relationship to the MDCDW.

IV. SUMMARY AND OUTLOOK

In this paper, we have discussed the Casimir energy produced by the quark field in the DCDW phase of quark matter under a magnetic field. We extended the Lifshitz formula to Dirac fermion fields in the MDCDW phase: our main formula is Eq. (11). Using this formula, we have calculated the Casimir energy in some parameter regions realizing the MDCDW phase.

In particular, we have examined the LL decomposition of the Casimir energy in a magnetic field. This analysis clarifies how each LL (among the LLLs and some types of HLLs) contributes to the total Casimir energy. The HLLs are classified by the presence or absence of FPs, as in Table I. Our findings may be summarized as, in the one-flavor case,

- LLL (weak eB): Singly oscillating Casimir effect.

- LLL (strong eB): Non-oscillating Casimir effect.

- (2,2)-type: Dually oscillating Casimir effect.

- (2,0)-type: Singly oscillating Casimir effect.

- (4,0)/Island-type: Dually oscillating Casimir effect.

- (0,0)-type: Sign-flipping Casimir effect.

Here, the "dual" effect in the (2,2)-type is caused by the spin-splitting, while that in the (4,0)/Island-type is attributed to the low-energy distortion of one dispersion relation. The situation of the two-flavor case is more complex, where the magnetic field splits the dispersion

---

[12] A similar system is the axion electrodynamics where the eigenvalues of modified photon fields in the $3 + 1$ dimensional spacetime are given as $\omega_{\zeta = \pm} = \sqrt{(\zeta\sqrt{\tilde{b}^2 + k_z^2} + \tilde{b})^2 + k_x^2 + k_y^2}$ with a parameter $\tilde{b}$. The sign-flipping Casimir effect originating from such photon fields was studied in Refs. [80, 82–87]. These dispersion relations correspond to $b = M \to \tilde{b}$ and $2|q_f B|l \to k_x^2 + k_y^2$ in our eigenvalues (7) at $\mu = 0$. Therefore, our finding is a new type of sign-flipping Casimir effect, which is induced by HLLs in the MDCDW phase.

relations of u, d quarks with different charges. As a result, we have observed the beating Casimir energy produced by u, d quarks.

Finally, we summarize our possible outlooks:

1. *Lattice simulations*—To examine the Casimir effect of interacting fermion systems, one can utilize numerical simulations of a lattice field theory (e.g., see Refs. [88–91] for the Casimir effect from Yang-Mills fields). In particular, the existence (or absence) of the MDCDW phase can be numerically tested by lattice NJL or QCD simulations. Although Monte-Carlo simulations are usually difficult at finite chemical potential due to the sign problem, the chemical potential required for the MDCDW phase is smaller than that of the DCDW phase in a zero magnetic field. Therefore, the lattice simulations of the Casimir effect in the MDCDW phase would be easier.

2. *Real kink crystals*—As another possible ground state within the NJL model, one can consider a solitonic modulation, the so-called real kink crystal (RKC) phase. The early references [46, 50, 55] predict that sufficiently strong magnetic fields tend to favor the MDCDW over the RKC (see Ref. [92] for analysis under only the RKC). The stability of the MDCDW phase is attributed to the spectral asymmetry of the LLLs in the MDCDW phase. However, in smaller magnetic fields (not dominated by only the LLLs), the RKC phase (or a hybridized phase [46]) may survive, and the Casimir effect in such a phase might be interesting.

3. *Chiral soliton lattice*—Apart from the NJL model, the chiral perturbation theory, which is an effective field theory of low-energy QCD based on mesonic degrees of freedom, predicts a ground state of magnetized finite-density QCD: the chiral soliton lattice (CSL) in QCD [93, 94], which is a stack of parallel π^0 domain walls. The MDCDW phase may be consistent with the CSL in the sense that it is induced by the Wess-Zumino-Witten-type anomaly [45, 46], while in the viewpoint of the Casimir effect, comparing the descriptions based on mesonic and quark degrees of freedom would be important.

4. *Dirac/Weyl semimetals*—In the typical dispersion relations of relativistic fermions in the three-dimensional Dirac/Weyl semimetals, Dirac/Weyl points are located at finite momenta (see Ref. [95, 96] for reviews). When a magnetic field is switched on, the low-energy spectrum of LLs can be distorted like those in Fig. 2, which is a remnant of Dirac/Weyl points. Since the typical behavior of the Casimir effect is characterized by the form of the dispersion relations, the classifications we suggested in this paper will be also useful for understanding the fermionic Casimir effect inside thin
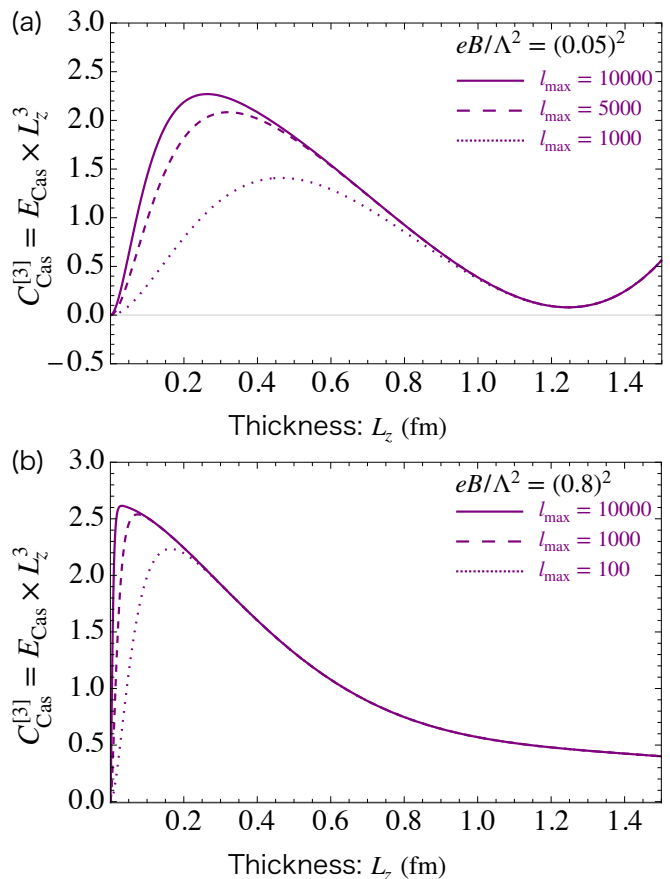

FIG. 7. l_{max} dependence of Casimir coefficient, where l_{max} is the maximum number of summed Landau levels. (a) the case in a weak magnetic field as in Fig. 4. (b) the case in a strong magnetic field as in Fig. 6.

films of Dirac/Weyl semimetals under a magnetic field (for analysis with only the LLL, see Ref. [24]).

Appendix A: Dependence on summation of LLs

In our numerical analysis in Sec. III, we summed LLs up to a maximum number l_{max}, which is large enough, and ignored higher levels. For the calculation of Casimir energy, this approximation is valid when L_z is long enough but is not sufficient when L_z is very short. In this Appendix, we examine the dependence of Casimir energy on l_{max}.

In Fig. 7, we compare some results by different l_{max}. Here, we show the total Casimir energy in the two-flavor MDCDW phase under a weak magnetic field [as in Fig. 4

(b)] or under a strong magnetic field [as in Fig. 6 (b)]. As shown in Fig. 7 (a), in a weak magnetic field, we can see that $l_{\max} = 1000$ is sufficient up to $L_z \sim 1.2$ fm while $l_{\max} = 5000$ is up to $L_z \sim 0.7$ fm. As shown in Fig. 7 (b), in a strong magnetic field, we can see that $l_{\max} = 5000$ and 10000 are sufficient up to $L_z \sim 0.1$ fm and near $L_z \sim 0$, respectively. Thus, if the magnetic field is strong enough, we can obtain almost exact results by summing many Landau levels.

Also, we find that, at $L_z \sim 0$, the results using a sufficient $l_{\max}$ approach to $C_{\mathrm{Cas}}^{[3]} = N_f N_c \times 2\pi^2/45$, where $2\pi^2/45$ is the factor known as the Casimir energy from the massless Dirac field in the 3+1 dimensional spacetime with the PBC in the z direction.

[1] H. B. G. Casimir, On the Attraction Between Two Perfectly Conducting Plates, Proc. Kon. Ned. Akad. Wetensch. **51**, 793 (1948).

[2] S. K. Lamoreaux, Demonstration of the Casimir Force in the 0.6 to $6\mu m$ Range, Phys. Rev. Lett. **78**, 5 (1997), [Erratum: Phys. Rev. Lett. **81**, 5475 (1998)].

[3] G. Bressi, G. Carugno, R. Onofrio, and G. Ruoso, Measurement of the Casimir force between parallel metallic surfaces, Phys. Rev. Lett. **88**, 041804 (2002), arXiv:quant-ph/0203002.

[4] G. Plunien, B. Müller, and W. Greiner, The Casimir Effect, Phys. Rep. **134**, 87 (1986).

[5] V. M. Mostepanenko and N. N. Trunov, The Casimir Effect and Its Applications, Sov. Phys. Usp. **31**, 965 (1988).

[6] M. Bordag, U. Mohideen, and V. M. Mostepanenko, New developments in the Casimir effect, Phys. Rep. **353**, 1 (2001), arXiv:quant-ph/0106045 [quant-ph].

[7] K. A. Milton, *The Casimir Effect: Physical Manifestations of Zero-Point Energy* (World Scientific, Singapore, 2001).

[8] G. L. Klimchitskaya, U. Mohideen, and V. M. Mostepanenko, The Casimir force between real materials: Experiment and theory, Rev. Mod. Phys. **81**, 1827 (2009), arXiv:0902.4022 [cond-mat.other].

[9] L. M. Woods, D. A. R. Dalvit, A. Tkatchenko, P. Rodriguez-Lopez, A. W. Rodriguez, and R. Podgornik, Materials perspective on Casimir and van der Waals interactions, Rev. Mod. Phys. **88**, 045003 (2016), arXiv:1509.03338 [cond-mat.mtrl-sci].

[10] T. Gong, M. R. Corrado, A. R. Mahbub, C. Shelden, and J. N. Munday, Recent progress in engineering the Casimir effect – applications to nanophotonics, nanomechanics, and chemistry, Nanophotonics **10**, 523 (2021).

[11] B.-S. Lu, The Casimir Effect in Topological Matter, Universe **7**, 237 (2021), arXiv:2105.11059 [cond-mat.mes-hall].

[12] K. Johnson, The M.I.T. Bag Model, Acta Phys. Pol. B **6**, 865 (1975).

[13] S. G. Mamaev and N. N. Trunov, Vacuum expectation values of the energy-momentum tensor of quantized fields on manifolds with different topologies and geometries. III, Sov. Phys. J. **23**, 551 (1980).

[14] I. E. Dzyaloshinskii, E. M. Lifshitz, and L. P. Pitaevskii, The general theory of van der Waals forces, Adv. Phys. **10**, 165 (1961).

[15] D. Robaschik, K. Scharnhorst, and E. Wieczorek, Radiative corrections to the Casimir pressure under the influence of temperature and external fields, Annals Phys. **174**, 401 (1987).

[16] M. V. Cougo-Pinto, C. Farina, and A. C. Tort, Fermionic Casimir effect in an external magnetic field, Conf. Proc. C **9809142**, 235 (1999), arXiv:hep-th/9809215.

[17] M. V. Cougo-Pinto, C. Farina, and A. C. Tort, The influence of an external magnetic field on the fermionic Casimir effect, Braz. J. Phys. **31**, 84 (2001).

[18] E. Elizalde, F. C. Santos, and A. C. Tort, Confined quantum fields under the influence of a uniform magnetic field, J. Phys. A **35**, 7403 (2002), arXiv:hep-th/0206143.

[19] M. Ostrowski, Casimir effect in external magnetic field, Acta Phys. Polon. B **37**, 1753 (2006), arXiv:hep-th/0504112.

[20] M. S. R. Miltao and F. A. Farias, The Casimir energy of Dirac field under a general boundary condition using the zeta function method, Acta Phys. Polon. B **39**, 1931 (2008).

[21] Y. A. Sitenko, Casimir effect with quantized charged spinor matter in background magnetic field, Phys. Rev. D **91**, 085012 (2015), arXiv:1411.2460 [hep-th].

[22] Y. A. Sitenko, Influence of quantized massive matter fields on the Casimir effect, Mod. Phys. Lett. A **30**, 1550099 (2015), arXiv:1506.05034 [hep-th].

[23] Y. A. Sitenko and S. A. Yushchenko, Pressure from the vacuum of confined spinor matter, Int. J. Mod. Phys. A **30**, 1550184 (2015), arXiv:1512.01397 [hep-th].

[24] K. Nakayama and K. Suzuki, Dirac/Weyl-node-induced oscillating Casimir effect, Phys. Lett. B **843**, 138017 (2023), arXiv:2207.14078 [cond-mat.mes-hall].

[25] A. Rohim, A. Romadani, and A. Salim Adam, Casimir effect of Lorentz-violating charged Dirac field in background magnetic field, Prog. Theor. Exp. Phys. **2024**, 033B01 (2024), arXiv:2307.04448 [hep-th].

[26] A. Erdas, Magnetic corrections to the fermionic Casimir effect in Horava-Lifshitz theories, Int. J. Mod. Phys. A **38**, 2350117 (2023), arXiv:2307.06228 [hep-th].

[27] A. Flachi, M. Nitta, S. Takada, and R. Yoshii, Fermion Casimir effect and magnetic Larkin-Ovchinnikov phases, (2024), arXiv:2410.18771 [hep-th].

[28] M. V. Cougo-Pinto, C. Farina, M. R. Negrao, and A. C. Tort, Bosonic Casimir effect in an external magnetic field, J. Phys. A **32**, 4457 (1999), arXiv:hep-th/9809214.

[29] M. V. Cougo-Pinto, C. Farina, M. R. Negrao, and A. C. Tort, Magnetic permeability of constrained scalar QED vacuum, Phys. Lett. B **483**, 144 (2000), arXiv:hep-th/9809216.

[30] M. V. Cougo-Pinto, C. Farina, M. R. Negrao, and A. Tort, Casimir effect at finite temperature of charged scalar field in an external magnetic field, (1998), arXiv:hep-th/9810033.

[31] M. V. Cougo-Pinto, C. Farina, and M. R. Negrao, Magnetic properties of confined bosonic vacuum at finite temperature, (1998), arXiv:hep-th/9811095.

[32] A. Erdas and K. P. Seltzer, Finite temperature Casimir

[32] effect for charged massless scalars in a magnetic field, Phys. Rev. D **88**, 105007 (2013), arXiv:1304.6417 [hep-th].

[33] A. Erdas and K. P. Seltzer, Finite temperature Casimir effect for massive scalars in a magnetic field, Int. J. Mod. Phys. A **29**, 1450091 (2014), arXiv:1312.1432 [hep-th].

[34] Y. A. Sitenko and S. A. Yushchenko, The Casimir effect with quantized charged scalar matter in background magnetic field, Int. J. Mod. Phys. A **29**, 1450052 (2014), arXiv:1401.6950 [hep-th].

[35] A. Erdas, Magnetic field corrections to the repulsive Casimir effect at finite temperature, Int. J. Mod. Phys. A **31**, 07 (2016), arXiv:1511.05940 [hep-th].

[36] A. Erdas, Casimir effect of a Lorentz-violating scalar in magnetic field, Int. J. Mod. Phys. A **35**, 2050209 (2020), arXiv:2005.07830 [hep-th].

[37] S. R. Haridev and P. Samantray, Revisiting vacuum energy in compact spacetimes, Phys. Lett. B **835**, 137489 (2022), arXiv:2106.12171 [hep-th].

[38] A. Erdas, Thermal effects on the Casimir energy of a Lorentz-violating scalar in magnetic field, Int. J. Mod. Phys. A **36**, 2150155 (2021), arXiv:2103.12823 [hep-th].

[39] A. Erdas, Casimir effect of a doubly Lorentz-violating scalar in magnetic field, (2024), arXiv:2408.13188 [hep-th].

[40] D. Fujii, K. Nakayama, and K. Suzuki, Dual chiral density wave induced oscillating Casimir effect, Phys. Rev. D **110**, 014039 (2024), arXiv:2402.17638 [hep-ph].

[41] F. Dautry and E. M. Nyman, Pion condensation and the σ-model in liquid neutron matter, Nucl. Phys. A **319**, 323 (1979).

[42] T. Tatsumi and E. Nakano, Dual chiral density wave in quark matter, arXiv:hep-ph/0408294.

[43] E. Nakano and T. Tatsumi, Chiral symmetry and density waves in quark matter, Phys. Rev. D **71**, 114006 (2005), arXiv:hep-ph/0411350.

[44] I. E. Frolov, V. C. Zhukovsky, and K. G. Klimenko, Chiral density waves in quark matter within the Nambu–Jona-Lasinio model in an external magnetic field, Phys. Rev. D **82**, 076002 (2010), arXiv:1007.2984 [hep-ph].

[45] T. Tatsumi, K. Nishiyama, and S. Karasawa, Novel Lifshitz point for chiral transition in the magnetic field, Phys. Lett. B **743**, 66 (2015), arXiv:1405.2155 [hep-ph].

[46] K. Nishiyama, S. Karasawa, and T. Tatsumi, Hybrid chiral condensate in the external magnetic field, Phys. Rev. D **92**, 036008 (2015), arXiv:1505.01928 [nucl-th].

[47] S. Carignano, E. J. Ferrer, V. de la Incera, and L. Paulucci, Crystalline chiral condensates as a component of compact stars, Phys. Rev. D **92**, 105018 (2015), arXiv:1505.05094 [nucl-th].

[48] E. J. Ferrer and V. de la Incera, Novel topological effects in dense QCD in a magnetic field, Nucl. Phys. B **931**, 192 (2018), arXiv:1512.03972 [nucl-th].

[49] E. J. Ferrer and V. de la Incera, Dissipationless Hall Current in Dense Quark Matter in a Magnetic Field, Phys. Lett. B **769**, 208 (2017), arXiv:1611.00660 [nucl-th].

[50] H. Abuki, Chiral crystallization in an external magnetic background: Chiral spiral versus real kink crystal, Phys. Rev. D **98**, 054006 (2018), arXiv:1808.05767 [hep-ph].

[51] E. J. Ferrer and V. de la Incera, Absence of Landau-Peierls Instability in the Magnetic Dual Chiral Density Wave Phase of Dense QCD, Phys. Rev. D **102**, 014010 (2020), arXiv:1902.06810 [nucl-th].

[52] B. Feng, E. J. Ferrer, and I. Portillo, Lack of Debye and Meissner screening in strongly magnetized quark matter at intermediate densities, Phys. Rev. D **101**, 056012 (2020), arXiv:2001.02617 [hep-ph].

[53] E. J. Ferrer and V. de la Incera, Axion-polaritons in the magnetic dual chiral density wave phase of dense QCD, Nucl. Phys. B **994**, 116307 (2023), arXiv:2010.02314 [hep-ph].

[54] E. J. Ferrer, V. de la Incera, and P. Sanson, Quark matter contribution to the heat capacity of magnetized neutron stars, Phys. Rev. D **103**, 123013 (2021), arXiv:2101.04032 [nucl-th].

[55] F. Anzuini and A. Melatos, Gradient expansion technique for inhomogeneous, magnetized quark matter, Eur. Phys. J. A **57**, 220 (2021), arXiv:2106.04744 [hep-ph].

[56] W. Gyory and V. de la Incera, Phase transitions and resilience of the magnetic dual chiral density wave phase at finite temperature and density, Phys. Rev. D **106**, 016011 (2022), arXiv:2203.14209 [nucl-th].

[57] E. J. Ferrer and A. Hackebill, Speed of sound for hadronic and quark phases in a magnetic field, Nucl. Phys. A **1031**, 122608 (2023), arXiv:2203.16576 [hep-ph].

[58] H. M. Ghalati and N. Sadooghi, Magnetic dual chiral density wave phase in rotating cold quark matter, Phys. Rev. D **108**, 054032 (2023), arXiv:2306.04472 [nucl-th].

[59] E. J. Ferrer, W. Gyory, and V. de la Incera, Thermal phonon fluctuations and stability of the magnetic dual chiral density wave phase in dense QCD, Phys. Rev. D **109**, 036023 (2024), arXiv:2307.05621 [nucl-th].

[60] E. J. Ferrer and V. de la Incera, Axion-polaritons in quark stars: a possible solution to the missing pulsar problem, Eur. Phys. J. C **84**, 133 (2024).

[61] E. J. Ferrer and V. de la Incera, Magnetic Dual Chiral Density Wave: A Candidate Quark Matter Phase for the Interior of Neutron Stars, Universe **7**, 458 (2021), arXiv:2201.04032 [hep-ph].

[62] Y. Nambu and G. Jona-Lasinio, Dynamical Model of Elementary Particles Based on an Analogy with Superconductivity. I, Phys. Rev. **122**, 345 (1961).

[63] Y. Nambu and G. Jona-Lasinio, Dynamical Model of Elementary Particles Based on an Analogy with Superconductivity. II, Phys. Rev. **124**, 246 (1961).

[64] U. Vogl and W. Weise, The Nambu and Jona-Lasinio model: Its implications for hadrons and nuclei, Prog. Part. Nucl. Phys. **27**, 195 (1991).

[65] S. P. Klevansky, The Nambu–Jona-Lasinio model of quantum chromodynamics, Rev. Mod. Phys. **64**, 649 (1992).

[66] T. Hatsuda and T. Kunihiro, QCD phenomenology based on a chiral effective Lagrangian, Phys. Rep. **247**, 221 (1994), arXiv:hep-ph/9401310.

[67] M. Buballa, NJL-model analysis of dense quark matter, Phys. Rep. **407**, 205 (2005), arXiv:hep-ph/0402234.

[68] E. M. Lifshitz, The theory of molecular attractive forces between solids, Sov. Phys. JETP **2**, 73 (1956).

[69] D. Fujii, K. Nakayama, and K. Suzuki, Lifshitz formulas for finite-density Casimir effect, (2024), arXiv:2408.08384 [quant-ph].

[70] A. Actor, I. Bender, and J. Reingruber, Casimir effect on a finite lattice, Fortschr. Phys. **48**, 303 (2000), arXiv:quant-ph/9908058 [quant-ph].

[71] M. Pawellek, Finite-sites corrections to the Casimir energy on a periodic lattice, arXiv:1303.4708 [hep-th].

[72] T. Ishikawa, K. Nakayama, and K. Suzuki, Casimir effect for lattice fermions, Phys. Lett. B **809**, 135713 (2020),

arXiv:2005.10758 [hep-lat].

[73] T. Ishikawa, K. Nakayama, and K. Suzuki, Lattice-fermionic Casimir effect and topological insulators, Phys. Rev. Res. **3**, 023201 (2021), arXiv:2012.11398 [hep-lat].

[74] K. Nakayama and K. Suzuki, Remnants of the nonrelativistic Casimir effect on the lattice, Phys. Rev. Res. **5**, L022054 (2023), arXiv:2204.12032 [quant-ph].

[75] K. Nakata and K. Suzuki, Magnonic Casimir Effect in Ferrimagnets, Phys. Rev. Lett. **130**, 096702 (2023), arXiv:2205.13802 [quant-ph].

[76] Y. V. Mandlecha and R. V. Gavai, Lattice fermionic Casimir effect in a slab bag and universality, Phys. Lett. B **835**, 137558 (2022), arXiv:2207.00889 [hep-lat].

[77] B. Swingle and M. Van Raamsdonk, Enhanced negative energy with a massless Dirac field, JHEP **08**, 183, arXiv:2212.02609 [hep-th].

[78] K. Nakata and K. Suzuki, Non-Hermitian Casimir effect of magnons, npj Spintronics **2**, 11 (2024), arXiv:2305.09231 [quant-ph].

[79] E. Flores, C. Ireland, N. Jamhour, V. Lasasso, N. Kurth, and M. Leinbach, Casimir force in discrete scalar fields I: 1D and 2D cases, arXiv:2309.00624 [quant-ph].

[80] K. Nakayama and K. Suzuki, Casimir effect in axion electrodynamics with lattice regularizations, Phys. Rev. D **109**, 065002 (2024), arXiv:2310.18092 [hep-th].

[81] C. W. J. Beenakker, Topologically protected Casimir effect for lattice fermions, Phys. Rev. Res. **6**, 023058 (2024), arXiv:2402.02477 [quant-ph].

[82] K. Fukushima, S. Imaki, and Z. Qiu, Anomalous Casimir effect in axion electrodynamics, Phys. Rev. D **100**, 045013 (2019), arXiv:1906.08975 [hep-th].

[83] I. Brevik, Axion Electrodynamics and the Axionic Casimir Effect, Universe **7**, 133 (2021), arXiv:2202.11152 [hep-ph].

[84] F. Canfora, D. Dudal, T. Oosthuyse, P. Pais, and L. Rosa, The Casimir effect in chiral media using path integral techniques, JHEP **09**, 095, arXiv:2207.09175 [hep-th].

[85] T. Oosthuyse and D. Dudal, Interplay between chiral media and perfect electromagnetic conductor plates: Repulsive vs. attractive Casimir force transitions, SciPost Phys. **15**, 213 (2023), arXiv:2301.12870 [hep-th].

[86] A. M. Favitta, I. H. Brevik, and M. M. Chaichian, Axion electrodynamics: Green's functions, zero-point energy and optical activity, Ann. Phys. (Amsterdam) **455**, 169396 (2023), arXiv:2302.13129 [hep-th].

[87] Y. Ema, M. Hazumi, H. Iizuka, K. Mukaida, and K. Nakayama, Zero Casimir force in axion electrodynamics and the search for a new force, Phys. Rev. D **108**, 016009 (2023), arXiv:2302.14676 [hep-ph].

[88] M. N. Chernodub, V. A. Goy, A. V. Molochkov, and H. H. Nguyen, Casimir Effect in Yang-Mills Theory in $D = 2 + 1$, Phys. Rev. Lett. **121**, 191601 (2018), arXiv:1805.11887 [hep-lat].

[89] M. N. Chernodub, V. A. Goy, and A. V. Molochkov, Phase structure of lattice Yang-Mills theory on $\mathbb{T}^2 \times \mathbb{R}^2$, Phys. Rev. D **99**, 074021 (2019), arXiv:1811.01550 [hep-lat].

[90] M. Kitazawa, S. Mogliacci, I. Kolbé, and W. A. Horowitz, Anisotropic pressure induced by finite-size effects in SU(3) Yang-Mills theory, Phys. Rev. D **99**, 094507 (2019), arXiv:1904.00241 [hep-lat].

[91] M. N. Chernodub, V. A. Goy, A. V. Molochkov, and A. S. Tanashkin, Boundary states and non-Abelian Casimir effect in lattice Yang-Mills theory, Phys. Rev. D **108**, 014515 (2023), arXiv:2302.00376 [hep-lat].

[92] G. Cao and A. Huang, Solitonic modulation and Lifshitz point in an external magnetic field within Nambu–Jona-Lasinio model, Phys. Rev. D **93**, 076007 (2016), arXiv:1601.03493 [nucl-th].

[93] D. T. Son and M. A. Stephanov, Axial anomaly and magnetism of nuclear and quark matter, Phys. Rev. D **77**, 014021 (2008), arXiv:0710.1084 [hep-ph].

[94] T. Brauner and N. Yamamoto, Chiral soliton lattice and charged pion condensation in strong magnetic fields, JHEP **04**, 132, arXiv:1609.05213 [hep-ph].

[95] N. P. Armitage, E. J. Mele, and A. Vishwanath, Weyl and Dirac Semimetals in three dimensional solids, Rev. Mod. Phys. **90**, 015001 (2018), arXiv:1705.01111 [cond-mat.str-el].

[96] B. Q. Lv, T. Qian, and H. Ding, Experimental perspective on three-dimensional topological semimetals, Rev. Mod. Phys. **93**, 025002 (2021).